



# Magma-sponge hypothesis and stratovolcanoes: Case for a compressible reservoir and quasi-steady deep influx at Soufrière Hills Volcano, Montserrat

Barry Voight,<sup>1</sup> Christina Widiwijayanti,<sup>1</sup> Glen Mattioli,<sup>2</sup> Derek Elsworth,<sup>1</sup> Dannie Hidayat,<sup>1</sup> and M. Strutt<sup>3</sup>

Received 10 November 2009; revised 23 December 2009; accepted 6 January 2010; published 18 February 2010.

[1] We use well-documented time histories of episodic GPS surface deformation and efflux of compressible magma to resolve apparent magma budget anomalies at Soufrière Hills volcano (SHV) on Montserrat, WI. We focus on data from 2003 to 2007, for an inflation succeeded by an episode of eruption-plus-deflation. We examine Mogi-type and vertical prolate ellipsoidal chamber geometries to accommodate both mineralogical constraints indicating a relatively shallow pre-eruption storage, and geodetic constraints inferring a deeper mean-pressure source. An exsolved phase involving several gas species greatly increases andesite magma compressibility to depths >10 km (i.e., for water content >4 wt%, crystallinity ~40%), and this property supports the concept that much of the magma transferred into or out of the crustal reservoir could be accommodated by compression or decompression of stored reservoir magma (i.e., the “magma-sponge”). Our results suggest quasi-steady deep, mainly mafic magma influx of the order of  $2 \text{ m}^3 \text{ s}^{-1}$ , and we conclude that magma released in eruptive episodes is approximately balanced by cumulative deep influx during the eruptive episode and the preceding inflation. Our magma-sponge model predicts that between 2003 and 2007 there was no evident depletion of magma reservoir volume at SHV, which comprises tens of  $\text{km}^3$  with radial dimensions of order ~1–2 km, in turn implying a long-lived eruption. **Citation:** Voight, B., C. Widiwijayanti, G. Mattioli, D. Elsworth, D. Hidayat, and M. Strutt (2010), Magma-sponge hypothesis and stratovolcanoes: Case for a compressible reservoir and quasi-steady deep influx at Soufrière Hills Volcano, Montserrat, *Geophys. Res. Lett.*, 37, L00E05, doi:10.1029/2009GL041732.

## 1. Introduction

[2] Resident magma in crustal magma reservoirs can be compressible. As a “magma sponge” it can in principle accommodate much of the volume of newly injected magma, with only part of the new magma being accommodated by expansion of the reservoir walls and consequent edifice inflation [Johnson, 1987, 1992; Johnson *et al.*, 2000]. Such

a mechanism has been proposed for a mafic reservoir under a basaltic shield volcano on Hawaii [Johnson, 1987; Johnson *et al.*, 2000], but application to intermediate to intermediate-silicic stratovolcano magmas is rare, partly because quasi-continuous geodetic network data and well-documented eruptive volume time-series records are available for only a few volcanoes. An unexcelled dataset derives from Soufrière Hills (SHV) volcano on Montserrat, WI, which has been erupting in pulsatory fashion since 1995, with a series of 2 to 3-year eruptive episodes and interspersed pauses lasting 1.5 to 2-years [Druitt and Kokelaar, 2002; Mattioli and Herd, 2003; Elsworth *et al.*, 2008]. These data provide controls on crustal processes contributing to stratovolcano behavior, and we use them to explore the role of magma-sponge reservoir storage and deeply sourced reservoir influxes on eruption periodicity.

## 2. Constraints at SHV

[3] The SHV has been investigated from 1995–present but the architecture of its magma storage zone remains enigmatic because some critical evidence is conflicting. The reservoir top has been reported at ~5 km (~115–130 MPa) based on phase equilibrium experiments and limited melt inclusion data on volatiles [Barclay *et al.*, 1998], hornblende phenocryst chemistry [Rutherford and Devine, 2003], and the deepest locations of volcano-tectonic earthquakes occurring near the conduit [Aspinall *et al.*, 1998]. Early GPS surface deformation data were interpreted to suggest a reservoir depth of ~6 km coupled to a deforming dike [Mattioli *et al.*, 1998], but post-1997 geodetic data supported a deeper source >9 km, assuming a spherical reservoir geometry [Mattioli and Herd, 2003; G. S. Mattioli *et al.*, GPS imaging of the SHV magma system from 1995 to 2008, submitted to *Geophysical Research Letters*, 2009]. The cumulative volume of the eruption, about  $1 \text{ km}^3$  DRE [Wadge *et al.*, 2010], and its chemical and petrological consistency over 14 years suggests that the andesite magma source is voluminous, several to tens of  $\text{km}^3$ . The response of borehole strainmeters to the major 2003 dome collapse further suggested a volatile-saturated magma body of several  $\text{km}^3$  with a top at 5–7 km depth [Voight *et al.*, 2006]. The mixed andesitic lavas require a deep supply of mafic magma [Murphy *et al.*, 2000]. Seismic imaging (B. Voight *et al.*, The SEA-CALIPSO volcano imaging experiment on Montserrat: Aims, plans, campaigns at sea and on land, and lessons learned, submitted to *Geophysical Research Letters*, 2009) has sought magma storage regions >5 km (E. Shalev *et al.*, Three-dimensional seismic velocity tomography of Mon-

<sup>1</sup>Earth and Mineral Sciences, Pennsylvania State University, University Park, Pennsylvania, USA.

<sup>2</sup>Department of Geosciences, University of Arkansas, Fayetteville, Arkansas, USA.

<sup>3</sup>British Geological Survey, Keyworth, UK.

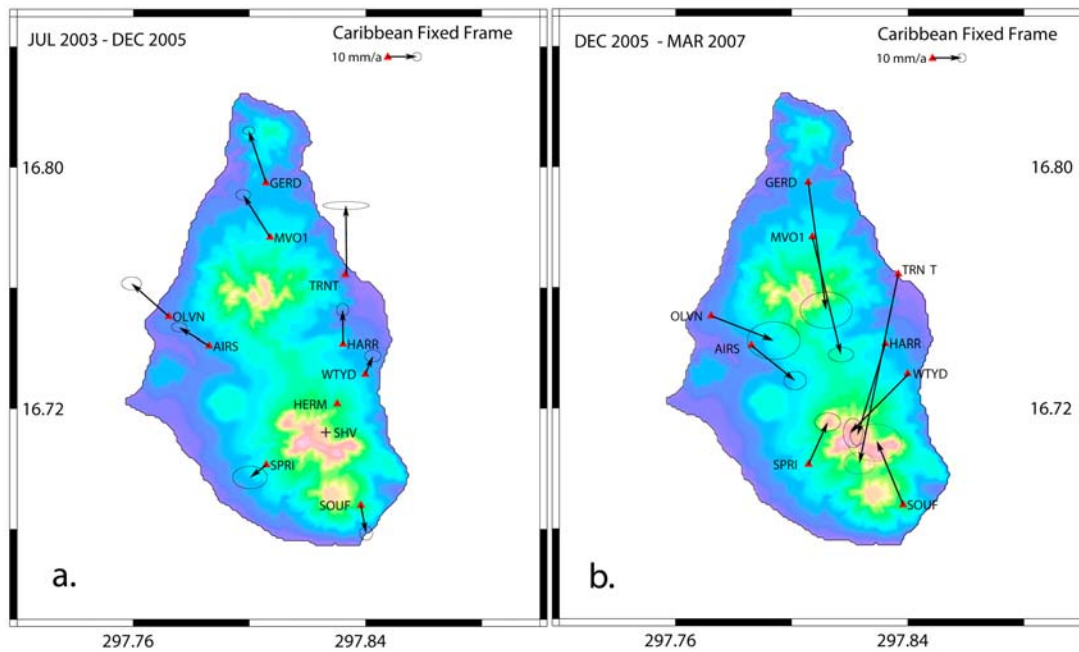


**Figure 1.** Maps of Soufrière Hills volcano showing the location of the eruptive vent (black cross labeled SHV), continuous GPS sites (red triangles) and the Caribbean-fixed GPS velocity vectors for the period (a) July 13, 2003 through December 1, 2005, and (b) December 2, 2005 through January 31, 2007, along with their 1-sigma error (ellipses for TRNT and SOUF were decreased by 50% in Figure 1b for clarity) for the cGPS sites. Note the strong radial deformation patterns corresponding to inflation in Figure 1a and deflation in Figure 1b.

tserrat from the SEA-CALIPSO offshore/onshore experiment, submitted to *Geophysical Research Letters*, 2009) but with poor resolution. A 2D seismic velocity section on a SE–NW line through SHV reveals a ~10 km-wide body with fast average velocity from the surface to >8 km depth [Paulatto *et al.*, 2010]. These results may be explained by crystallized intrusions and host rock precipitation of silica and hydrothermal minerals, with currently-active magma storage region(s) contained inside this body but masked at the seismic resolution.

[4] Thus the strongest constraints on reservoir architecture may be from geodetic imaging. Here we examine the merits of an internally stratified, single crustal reservoir with top below 5 km bsl and centroid near 10 km, whose geometry is possibly vertically-elongated, and whose base is supplied by a deep factory for intermediate to mafic hydrous melts at least partly fractionated near and above the crust-mantle boundary [Voight *et al.*, 2008]. The model presented here is an alternative to others that have been proposed. Notably, Mattioli *et al.* [1998] modeled 1995–97 surface deformation from GPS geodesy as a halfspace with two sources of deformation, a Mogi-type source at ~6 km, and a shallower NW-trending dike. Subsequent solutions, conditioned by post-1999 data which are both spatially and temporally denser, favored a deeper spherical source (G. S. Mattioli *et al.*, Long term surface deformation of Soufrière Hills Volcano, Montserrat from GPS geodesy: Inferences from simple elastic inverse models, manuscript in preparation, 2009). This led Elsworth *et al.* [2008] to propose a model with two stacked magma reservoirs, at depths of 6 km and 12 km, connected from surface to deep crust and mantle by vertical conduits; GPS velocities were co-inverted with

surface efflux to calculate magma transfer rates through intermediate and deep crust. These results differ substantially from the model presented here, as discussed below.

### 3. Data and Modeling

[5] Surface deformation associated with the ongoing eruption of SHV was measured initially using campaign GPS beginning in 1995, with the earliest observations acquired 6 weeks prior to quasi-continuous andesite extrusion in November [Mattioli *et al.*, 1998]. Since 1996 a network of continuous GPS (cGPS) sites has operated, with the current network (post-2003) comprised of 10 sites located at radial distances between 1.6 and 9.6 km from the center of activity [Mattioli *et al.*, 2004, also submitted manuscript, 2009].

[6] It is convenient to consider episodes of ground inflation and deflation in pairs, with each inflation followed by a succeeding eruption and concurrent deflation. The initial inflation is inferred to have occurred between 1992–1995, but surface deformation observations at SHV only began in August 1995 [Mattioli *et al.*, 1998]. The initial poorly observed epoch was followed in Nov 1995 by the first of three distinct episodes of surface subsidence recorded by GPS at SHV, which correspond to a deflating crustal source and active surface efflux, separated by surface uplifts that correlate with inflating sources and observed pauses in surface activity [Elsworth *et al.*, 2008; Mattioli *et al.*, submitted manuscript, 2009]. Caribbean-fixed velocities reveal radial displacements toward the volcanic source during deflations, and away from the source during inflations (Figure 1). Here we focus on a representative pair of inflations and deflations, from 13 July 2003–01 Nov 2005, and 02 Nov 2005–31 Jan

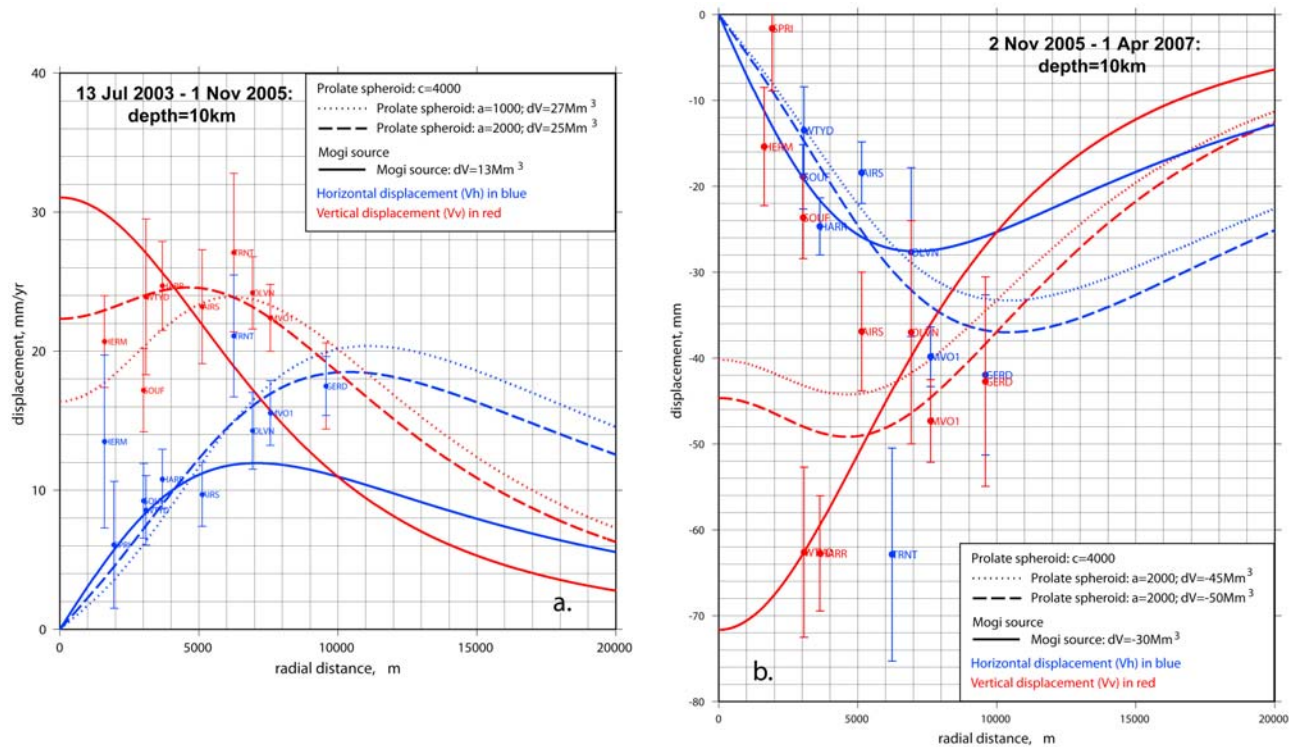


**Figure 2.** Vertical and horizontal radial displacements against radial distance from vent. (a) The 2003–05 inflation episode and (b) the 2005–07 deflation episode, with GPS data corrected for lava dome loading [Poulos and Davis, 1994]. Data compared to forward Mogi and prolate spheroid models for centroid depth 10 km, with volume changes as specified.

2007, respectively, which encompass the strengthened post-Feb 2003 cGPS network [Mattioli *et al.*, 2004, also submitted manuscript, 2009]. Horizontal and vertical ground displacements (and error bars) with radial distance from the vent for the two cases are shown in Figure 2.

[7] First we consider the 2005–2007 deflation (Figure 2b), in order to directly compare ground deformation to erupted volume. Our cGPS data have been adjusted to correct for surface load effects related to emplacement of dome lava during this episode, 205  $\text{Mm}^3$  assuming a density of  $2100 \text{ kg/m}^3$  [Poulos and Davis, 1994]. The plot compares the adjusted cGPS data to results from elastic analytical models. Elastic response is inferred from observed constant rates of surface deformation during inflation and deflation, and rapid changes in deformation sense that are synchronous with the efflux record (see auxiliary material).<sup>1</sup> A point source, embedded in an elastic half-space and using uncorrected data, excluding HERM which is significantly affected by dome loading, yields an inverted centroid depth as 10.3 km and a reservoir volume change  $DVr$  of  $-44.2 \text{ Mm}^3$  [Delaney and McTigue, 1994] (see auxiliary material). Manual fits to the same displacement data were of similar or superior fidelity [Mattioli *et al.*, 1998, also submitted manuscript, 2009] (see auxiliary material) representing a spherical source at nominal depth 10.0 km and  $DVr = -30.0 \text{ Mm}^3$ . In contrast, the measured volume of erupted material during this epoch was  $316 \text{ Mm}^3$  DRE (MVO data [Wadge *et al.*, 2010]).

[8] Data for the preceding inflation epoch, 13 July 2003–01 Nov 2005 (Figures 1a and 2b) are compared in Figure 2

(no load corrections required in this case since the dome was already removed) to results from analytical models. A point source [Mogi, 1958], embedded in an elastic half-space under the vent and excluding the proximal HERM site, yields an inverted centroid depth as 10.4 km and a reservoir volume change  $DVr$  of  $16.8 \text{ Mm}^3$ . Again, forward models yield a spherical source at nominal depth 10.0 km and  $DVr = 16.0 \text{ Mm}^3$ .

[9] We also explored alternative geometries of vertical prolate-ellipsoids centered from 6 to 14 km and variable aspect ratios. Figure 2b shows the forward models with  $Z = 10.0$ ,  $c = 4.0$ ,  $a = 2.0, 2.4 \text{ km}$ , identical to that used in Figure 2a, and  $DVr = 23\text{--}25 \text{ Mm}^3$ . The vertical elongation model appears supported by the 2003–05 GPS data, which display a central dimple of vertical displacement better fit by this model close to the conduit (Figure 2a).

[10] Now we address magma volumes and magma compressibility. The compressibility  $C$  of saturated magma plus exsolved gas, which is the inverse of effective bulk modulus  $\beta$ , greatly exceeds host rock. Following the relations of Huppert and Woods [2002], and assuming exsolution occurs at chemical and thermodynamic equilibrium (valid for slow processes), the exsolved volatile content,  $n$ , derives from Henry's Law. Assuming water is the dominant volatile species, this law is  $n = N - sp^{1/2}(1-x) > 0$ , for saturated magma, where  $N$  is water content, Henry's law constant  $s = 4.1 \times 10^{-6} \text{ Pa}^{-1/2}$  for  $\text{H}_2\text{O}$  vapor,  $p$  is pressure, and  $x$  is crystal content (further details are in the auxiliary material). Assuming  $N = 5 \text{ wt}\%$  we calculate for a magma chamber depth of 10 km ( $\pm 4 \text{ km}$ ) an average  $C = 1/\beta = 7.58 \times 10^{-10} \text{ Pa}^{-1}$ , and average  $\beta = 1.32 \times 10^9 \text{ Pa}$ . The assumption of  $N = 5 \text{ wt}\%$  is justified by data from Barclay *et al.* [1998], who reported

<sup>1</sup>Auxiliary materials are available in the HTML. doi:10.1029/2009GL041732.

as much as 5.05 wt % H<sub>2</sub>O from melt inclusions in 1996 SHV lavas and pumice, and by recent data, which have revealed  $N > 6$  wt % in pumice glass samples [Edmonds *et al.*, 2008]. The evidence also suggests an excess vapor phase at depth that includes appreciable CO<sub>2</sub> and SO<sub>2</sub>. The range in CO<sub>2</sub>-H<sub>2</sub>O in melt inclusions in pumice is consistent with an exsolved CO<sub>2</sub>-rich vapor phase to pressures >400 MPa [Edmonds *et al.*, 2008]. The significance of these observations is that exsolved volatile phases in addition to H<sub>2</sub>O are available to enhance compressibility of magma at depth.

[11] Next we correct for the injected (or discharged) magma volume  $DV_{\text{dm}}$  and the deflected reservoir wall volume change  $DV_r$  [Johnson, 1992; Johnson *et al.*, 2000], as  $DV_{\text{dm}}/DV_r = \{1 + 4\mu/3\beta\}$ , where  $\mu$  is shear modulus of the host rock, and  $\beta$  is the effective bulk modulus of resident magma in the reservoir. We assume  $\mu = 5.0 \times 10^9$  Pa [Elsworth *et al.*, 2008], yielding a  $DV_{\text{dm}}/DV_r = 6.0$ .

[12] Now we apply this relation to the 2005–2007 eruption-deflation episode. The spherical forward model gave  $DV_r = -30 \text{ Mm}^3$  for volume change of the source cavity, suggesting a corresponding volume of magma withdrawn from the reservoir of  $-30 \times 6.0 = -180 \text{ Mm}^3$ . The measured volume of erupted lava during this deflation was  $316 \text{ Mm}^3$  DRE (MVO data). The difference is  $136 \text{ Mm}^3$ , which can be accounted for by injection into the reservoir from a deep source over the course of the episode, with corresponding discharge of an equivalent volume. The average deep influx for this episode is thus  $136 \text{ Mm}^3 / 4.557 \times 10^7 \text{ s} = 2.98 \text{ m}^3/\text{s}$ . An ellipsoidal model cannot be evaluated strictly with this equation, but as a very rough estimate the implication is a discharged volume of  $-40 \times 6.0 = -240 \text{ Mm}^3$ , a difference of  $76 \text{ Mm}^3$  with erupted lava, and a deep influx of  $\sim 1.6 \text{ m}^3/\text{s}$ .

[13] For the preceding 2003–2005 inflation, the sphere inversion model gave  $DV_r = 16.8 \text{ Mm}^3$  for volume change of the source cavity, suggesting a corresponding volume of magma intruded into the reservoir of  $16.8 \times 6.0 = 100.8 \text{ Mm}^3$ . The average deep influx for this epoch is thus  $100.8 \text{ Mm}^3 / 7.271 \times 10^7 \text{ s} = 2.00 \text{ m}^3/\text{s}$ . As a rough estimate the ellipsoid model suggests a deep influx of  $2.6 \text{ m}^3/\text{s}$ . The steadiness of this calculated magma input, the small magnitudes of input relative to the chamber volume (maybe 0.1% replenishment over 2 years), and the apparent linearity of the volume changes in time (see auxiliary material) suggest that chamber total pressures do not significantly change, and that compressibility as influenced by total pressure and composition stays approximately constant.

#### 4. Discussion

[14] The pressure in the reservoir is assumed to increase due to influx of deep magma [cf. Blake, 1981] and through fractional crystallization and volatile oversaturation [Blake, 1984; Tait *et al.*, 1989; Blundy *et al.*, 2006]. In our view the eruption phase is triggered when overpressure reaches a critical value with respect to wall rock tensile strength (a value dependent on reservoir geometry and ambient wall-rock stress state), and a dike toward the surface is generated (or reopened), although its geometry may be modified near the surface [Costa *et al.*, 2007]. The pulsatory behavior of the SHV eruption, reflected in the GPS pattern, indicates a repetition of the process with waxing and waning of reservoir overpressure. With volatile saturated magma containing exsolved bubbles of vapor, the mixture is compressible and

reservoir overpressure is only relieved when a significant part (perhaps 1 to 10%) of the reservoir mass is erupted [Bower and Woods, 1998], ignoring any additional deep influx. With relief of overpressure, the conduit seals and the eruption phase is paused. Edifice inflation begins again with a pause in surface efflux, and when overpressure has rebuilt to a critical threshold due to continued deep influx and crystallization, a dike reopens, and an eruptive episode restarts. At present at SHV, three complete 2–3 year cycles of inflation and succeeding eruption/deflation have occurred. A fourth inflation began in April 2007. Thus the current magma reservoir and eruption comprises materials injected since 1992 plus older, partly-molten andesitic materials capable of being remobilized by new hot, volatile rich magma. The upper part of the reservoir contains crystal-rich, highly viscous, gas-saturated, rhyolitic melt (similar to erupted lava), overlying a lower part of crystal-poorer less-viscous but hydrous intermediate to mafic magmas [cf. Annen *et al.*, 2006; Zellmer *et al.*, 2003]. Our models suggest magma is stored in a reservoir centered around 10 km depth, but whose top may be several km shallower in accordance with petrological criteria [Barclay *et al.*, 1998].

[15] Primary aspects of our model are that (1) an exsolved gas phase primarily involving H<sub>2</sub>O, CO<sub>2</sub> and SO<sub>2</sub> greatly increases magma compressibility, suggesting that most of the magma volume transferred into or out of the reservoir is accommodated by compression or decompression of stored reservoir magma rather than by quasi-elastic deflection of reservoir walls, and (2) deep influx is both continuous and nearly steady. With respect to (1), our calculations suggest that about 48% of the volume of magma removed from the reservoir in 2005–07 was accommodated by decompression of resident reservoir magma, with 42% recharged by deep influx in 2005–07, and only 10% by inward deflection of the reservoir walls. For the inflation episode of 2003–05, about 83% of the volume of magma injected into the reservoir was accommodated by compression of resident magma, with the remaining 17% taken up by outward deflection of reservoir walls. Johnson [1992] and Johnson *et al.* [2000] reported comparable numbers for Kilauea volcano for the 1983–1986 Pu'u 'O'o basalt eruption, with only 20–25% by volume accommodated by chamber enlargement, and the rest by compression or decompression of stored magma.

[16] With respect to point (2), in both inflation and deflation episodes our results suggest deep influx of the order of  $2 \text{ m}^3/\text{s}$ , consistent with a steady-state process. The long-term average eruption rate from July 1995 to July 2009 is  $1.8 \text{ m}^3/\text{s}$  DRE (MVO data).

[17] Finally, estimates of resident reservoir volume appear feasible. A simple approach is to assume bubble compression accounts for accommodation of injected or released magma from the chamber. Assuming bubble porosity of the order  $\sim 1$  vol% [e.g., Voight *et al.*, 2006], our estimate of  $180 \text{ Mm}^3$  for decompression-released magma in 2005–07 yields a spherical chamber radius of 1.6 km, or for a cylindrical reservoir from 6–14 km, a radius of 0.85 km. Considerations of magma crystallinity increase these values; a crystal fraction of 0.4 yields sphere radius of 2.2 km, and cylinder radius 1.3 km. The reservoir volume thus is of order of tens of cubic kilometers. Our model appears consistent with both mineralogical constraints indicating shallow storage of some erupted lava, GPS indications of a deeper mean-pressure source when the full reservoir expands or

contracts, and magma budget anomalies. The presence of an exsolved gas phase involving multiple species greatly increases magma compressibility to depths >10 km and suggests that most of the magma volume transferred into or out of the reservoir can be accommodated by compression or decompression of stored reservoir magma with radial dimensions of ~1–2 km.

## 5. Conclusions

[18] We use well-documented time histories of pulsatory GPS-derived surface deformation and magma efflux to geodetically image magma storage and transfer within the deep crustal system of the Soufrière Hills volcano from 2003 to 2007, with an inflation succeeded by an episode of eruption-plus-deflation. The spherical and prolate ellipsoidal models presented here contrast with the vertically stacked dual-Mogi-type geometry favored by *Elsworth et al.* [2008]. The ellipsoid model, a geometrical idealization for a vertically-elongated shape that can be more complex, better incorporates mineralogical and phase equilibrium constraints indicating relatively shallow storage of erupted lava and GPS-derived surface deformation for the single epoch of eruption and repose (Mattioli et al., submitted manuscript, 2009) that implies a deeper mean-pressure source when the full reservoir deforms. The presence of an exsolved gas phase involving several species greatly increases magma compressibility to depths >10 km, and supports the concept that most of the magma volume transferred into or out of the mid-crustal reservoir can be accommodated by compression or decompression of *in situ* reservoir magma, which we term the magma-sponge. For both inflation and deflation epochs our results suggest quasi-steady deep, largely mafic magma influx of the order of  $2 \text{ m}^3 \text{ s}^{-1}$ . We conclude that the magma released in eruptive episodes is approximately balanced by the accumulated deep influx of the eruptive episode and the preceding inflation. For this model there is no evident depletion of magma reservoir volume through 2007, which comprises tens of  $\text{km}^3$  with radial dimensions of order ~1–2 km.

[19] **Acknowledgments.** This research was supported by NSF/EAR Continental Dynamics, and Instrumentation and Facilities, and our Universities. MVO colleagues provided field support. We are grateful to support from our CALIPSO Consortium colleagues.

## References

Annen, C., et al. (2006), The genesis of intermediate and silicic magmas in deep crustal hot zones, *J. Petrol.*, *47*, 505–540, doi:10.1093/petrology/egi084.

Aspinall, W. P., et al. (1998), Soufrière Hills eruption, Montserrat, 1995–1997: Volcanic earthquake locations and fault plane solutions, *Geophys. Res. Lett.*, *25*, 3397–3400, doi:10.1029/98GL00858.

Barclay, J., et al. (1998), Experimental phase equilibria constraints on pre-eruptive storage conditions of the Soufrière Hills magma, *Geophys. Res. Lett.*, *25*, 3437–3440, doi:10.1029/98GL00856.

Blake, S. (1981), Volcanism and the dynamics of open magma chambers, *Nature*, *289*, 783–785, doi:10.1038/289783a0.

Blake, S. (1984), Volatile oversaturation during the evolution of silicic magma chambers as an eruption trigger, *J. Geophys. Res.*, *89*, 8237–8244, doi:10.1029/JB089iB10p08237.

Blundy, J., et al. (2006), Magma heating by decompression-driven crystallization beneath andesite volcanoes, *Nature*, *443*, 76–80, doi:10.1038/nature05100.

Bower, S. M., and A. W. Woods (1998), On the influence of magma chambers controlling the evolution of explosive volcanic eruptions, *J. Volcanol. Geotherm. Res.*, *86*, 67–78, doi:10.1016/S0377-0273(98)00081-X.

Costa, A., O. Melnik, R. S. J. Sparks, and B. Voight (2007), Control of magma flow in dykes on cyclic lava dome extrusion, *Geophys. Res. Lett.*, *34*, L02303, doi:10.1029/2006GL027466.

Delaney, P. T., and D. F. McTigue (1994), Volume of magma accumulation or withdrawal estimated from surface uplift or subsidence, with application to the 1960 collapse of Kilauea Volcano, *Bull. Volcanol.*, *56*, 417–424, doi:10.1007/BF00302823.

Druitt, T. H., and P. Kokelaar (Eds.) (2002), *The Eruption of Soufrière Hills Volcano, From 1995 to 1999*, *Geol. Soc. London Mem.*, *21*, 645 pp.

Edmonds, M., et al. (2008), Bulk volatile concentration in the Soufrière Hills Volcano magma prior to eruption, paper presented at the IAVCEI General Assembly, Eur. Sci. Found., Reykjavik.

Elsworth, D., et al. (2008), Implications of magma transfer between multiple reservoirs on eruption cycling, *Science*, *322*, 246–248, doi:10.1126/science.1161297.

Huppert, H. E., and A. W. Woods (2002), The role of volatiles in magma chamber dynamics, *Nature*, *420*, 493–495, doi:10.1038/nature01211.

Johnson, D. J. (1987), Elastic and inelastic magma storage at Kilauea volcano, *U.S. Geol. Surv. Prof. Pap.*, *1350*, 1297–1306.

Johnson, D. J. (1992), Dynamics of magma storage in the summit reservoir of Kilauea Volcano, Hawaii, *J. Geophys. Res.*, *97*, 1807–1820, doi:10.1029/91JB02839.

Johnson, D. J., et al. (2000), Comment on “Volume of magma accumulation or withdrawal estimated from surface uplift or subsidence, with application to the 1960 collapse of Kilauea volcano” by P. T. Delaney and D. F. McTigue, *Bull. Volcanol.*, *61*, 491–493, doi:10.1007/s004450050006.

Mattioli, G. S., and R. Herd (2003), Correlation of cyclic surface deformation recorded by GPS geodesy with surface magma flux at Soufrière Hills Volcano, Montserrat, *Seismol. Res. Lett.*, *74*, 230.

Mattioli, G. S., et al. (1998), GPS measurement of surface deformation around Soufrière Hills volcano, Montserrat, from October 1995 to July 1996, *Geophys. Res. Lett.*, *25*, 3417–3420, doi:10.1029/98GL00931.

Mattioli, G. S., et al. (2004), Prototype PBO instrumentation of CALIPSO Project captures world-record lava dome collapse on Montserrat, *Eos Trans. AGU*, *85*(34), doi:10.1029/2004EO340001.

Mogi, K. (1958), Relations between the eruptions of various volcanoes and the deformations of the ground surfaces around them, *Bull. Earthquake Res. Inst. Univ. Tokyo*, *36*, 99–134.

Murphy, M. D., et al. (2000), Remobilization of andesite magma by intrusion of mafic magma at the Soufrière Hills volcano, Montserrat, West Indies, *J. Petrol.*, *41*, 21–42, doi:10.1093/petrology/41.1.21.

Paulatso, M., T. A. Minshull, and T. J. Henstock (2010), Constraints on an intrusive system beneath the Soufrière Hills Volcano, Montserrat, from finite difference modeling of a controlled source seismic experiment, *Geophys. Res. Lett.*, doi:10.1029/2009GL041805, in press.

Poulos, H. G., and E. H. Davis (1994), *Elastic Solutions for Soil and Rock Mechanics*, 411 pp., John Wiley, Hoboken, N. J.

Rutherford, M. J., and J. D. Devine (2003), Magmatic conditions and magma ascent as indicated by hornblende phase equilibria and reaction in the 1995–2002 Soufrière Hills magma, *J. Petrol.*, *44*, 1433–1454, doi:10.1093/petrology/44.8.1433.

Tait, S., et al. (1989), Pressure, gas content, and eruption periodicity of a shallow, crystallizing magma chamber, *Earth Planet. Sci. Lett.*, *92*, 107–123, doi:10.1016/0012-821X(89)90025-3.

Voight, B., et al. (2006), Unprecedented pressure increase in deep magma reservoir triggered by lava-dome collapse, *Geophys. Res. Lett.*, *33*, L03312, doi:10.1029/2005GL024870.

Voight, B., et al. (2008), Conundrum on magmatic reservoir of Soufrière Hills volcano, Montserrat: enigmatic evidence and the case for a vertically-elongated reservoir, *Eos Trans. AGU*, *89*(53), Fall Meet. Suppl., Abstract V53C-0X.

Wadge, G., R. Herd, G. Ryan, E. S. Calder, and J.-C. Komorowski (2010), Lava production at Soufrière Hills Volcano, Montserrat: 1995–2009, *Geophys. Res. Lett.*, doi:10.1029/2009GL041466, in press.

Zellmer, G. F., et al. (2003), Magma emplacement and remobilization time-scales beneath Montserrat: Insights from Sr and Ba zonation in plagioclase phenocrysts, *J. Petrol.*, *44*, 1413–1432, doi:10.1093/petrology/44.8.1413.

D. Elsworth, D. Hidayat, B. Voight, and C. Widiwijayanti, Earth and Mineral Sciences, Pennsylvania State University, Deike Bldg., University Park, PA 16802, USA. (voight@ems.psu.edu)

G. Mattioli, Department of Geosciences, University of Arkansas, 113 Ozark Hall, Fayetteville, AR 72701, USA.

M. Strutt, British Geological Survey, Keyworth NG12 5GG, UK.